ELSEVIER

Contents lists available at ScienceDirect

# Journal of Hazardous Materials

journal homepage: www.elsevier.com/locate/jhazmat





# Advances in antimicrobial activity analysis of fluoroquinolone, macrolide, sulfonamide, and tetracycline antibiotics for environmental applications through improved bacteria selection

Ethan Hain a, Hollie Adejumo a,b, Bridget Anger a, Joseph Orenstein a, Lee Blaney a,\*

- <sup>a</sup> University of Maryland Baltimore County, Department of Chemical, Biochemical, and Environmental Engineering, 1000 Hilltop Circle, Engineering 314, Baltimore, MD 21250, USA
- b University of Michigan, Department of Civil and Environmental Engineering, 2350 Hayward Street, 2105 GG Brown Building, Ann Arbor, MI 48109-2125, USA

#### ARTICLE INFO

Editor: Dr. R. Debora

Keywords:
Half-maximal inhibitory concentration (IC<sub>50</sub>)
Minimum inhibitory concentration (MIC)
Contaminants of emerging concern
Pharmaceutical
Bioassay

#### ABSTRACT

The widespread use of antibiotics has led to their ubiquitous presence in water and wastewater and raised concerns about antimicrobial resistance. Clinical antibiotic susceptibility assays have been repurposed to measure removal of antimicrobial activity during water and wastewater treatment processes. The corresponding protocols have mainly employed growth inhibition of *Escherichia coli*. The present work focused on optimizing bacteria selection to improve the sensitivity of residual antimicrobial activity measurements by broth microdilution assays. Thirteen antibiotics from four classes (*i.e.*, fluoroquinolones, macrolides, sulfonamides, tetracyclines) were investigated against three gram-negative organisms, namely *E. coli*, *Mycoplasma microti*, and *Pseudomonas fluorescens*. The minimum inhibitory concentration (MIC) and half-maximal inhibitory concentration (IC<sub>50</sub>) were calculated for each antibiotic-bacteria pair. *P. fluorescens* produces a fluorescent siderophore, pyoverdine, that was used to assess sublethal effects and further enhance the sensitivity of antimicrobial activity measurements. The optimal antibiotic-bacteria pairs were as follows: fluoroquinolone-*E. coli* (growth inhibition); macrolide- and sulfonamide-*M. microti* (growth inhibition); and, tetracycline-*P. fluorescens* (pyoverdine inhibition). Compared to *E. coli* growth inhibition, the sensitivity of antimicrobial activity analysis was improved by up to 728, 19, and 2.7 times for macrolides (tylosin), sulfonamides (sulfamethoxazole), and tetracyclines (chlortetracycline), facilitating application of these bioassays at environmentally-relevant conditions.

#### 1. Introduction

Antibiotics have been ubiquitously detected in finished drinking water, treated wastewater effluent, animal manure, and surface water (Tahrani et al., 2016; Hopanna et al., 2020; Zhang et al., 2029; Zhang et al., 2019; Van Epps and Blaney, 2016; He et al., 2019; Barbosa et al., 2018; He and Blaney, 2015) and, consequently, contribute to global public health concerns associated with the development and spread of antimicrobial resistance (Karkman et al., 2016; Su et al., 2018) or other ecological effects (Jepsen et al., 2019). In water and wastewater treatment processes, select antibiotics (e.g., fluoroquinolones, macrolides, sulfonamides, and tetracyclines) are not fully mineralized, but rather partially degraded into various transformation products (He et al., 2015; Postigo and Richardson, 2014). Many of the transformation products have been identified as known antibiotics (Wammer et al., 2006;

Snowberger et al., 2016; Chen et al., 2019). For example, Snowberger et al. (2016) demonstrated that UV irradiation at 254 nm, which is used for disinfection in both drinking water and wastewater treatment, transforms select fluoroquinolone antibiotics into other marketed fluoroquinolones. Other transformation products may also retain antimicrobial activity (Dodd et al., 2009; Baeza and Knappe, 2011). To measure the potency of parent antibiotics or the residual antimicrobial activity of treated water or wastewater, the following techniques have been employed: agar dilution (Szabó et al., 2017); broth micro- (Dodd et al., 2009) and macro-dilution (Hacek et al., 1999); disk diffusion (Koczura et al., 2012); and, the Etest (Sekizuka et al., 2019). Of these approaches, the broth microdilution assay described by the Clinical and Laboratory Standards Institute (CLSI) (CLSI, 2016) is commonly performed due to the straightforward protocol and ease of replication (Luber et al., 2003; Schumacher et al., 2018); however, this approach

E-mail address: blaney@umbc.edu (L. Blaney).

 $<sup>^{\</sup>ast}$  Corresponding author.

has not been optimized for assessment of antimicrobial activity specific to environmental applications.

The broth microdilution protocol relates antibiotic concentration and bacterial growth (CLSI, 2016). To run the assay, a solution containing a particular antibiotic is mixed with a bacterial inoculum at a 1:1 ratio in a microplate well. The antibiotic solution is serially diluted to achieve a range of antibiotic concentrations (i.e., dose), and the optical density of the bacteria (i.e., response) is recorded after 16-20 h of exposure. Following the standard CLSI protocol (CLSI, 2016), broth microdilution assays are used to identify the minimum inhibitory concentration (MIC) for a particular antibiotic-bacteria pair. The MIC is the lowest antibiotic concentration that prevents visible bacterial growth in the microplate well (Witebsky et al., 1979) and, therefore, serves as a conservative estimate of the antibiotic concentration needed to inhibit growth (Reller et al., 2009). However, specific assay protocols influence the observed MIC, and individual researchers can interpret visible growth using different scales (Hain et al., 2018). To better quantify residual antimicrobial activity for environmental applications, more accurate and precise growth inhibition parameters are needed. For these reasons, the Hill equation has been leveraged to fit dose-response relationships and calculate half-maximal inhibitory concentrations (IC<sub>50</sub> values) (Goutelle et al., 2008). The IC<sub>50</sub> values serve as reproducible benchmarks of antimicrobial activity and can be used to understand the relative potency of antibiotics that have been detected in the

Antibiotics exhibit variable potency against different bacteria species, as indicated in Table S1 (MIC values) and Table S2 (IC50 parameters) of the Supporting Information (SI). Fluoroquinolone antibiotics were generally potent against all of the bacteria listed in Tables S1-S2 of the SI. Macrolides were more potent against Mycoplasma spp. (Table S1 in the SI) but displayed inconsistent activity against different species. For example, the MIC of erythromycin was 8  $\mu g L^{-1}$  for Mycoplasma pneumoniae (Wei et al., 2019) and greater than 8000 µg L<sup>-1</sup> for Mycoplasma synoviae (Catania et al., 2019). Some antibiotics were ineffective for particular bacteria. For instance, the IC50 values of sulfachloropyridazine, sulfadimethoxine, and sulfamethoxazole for Pseudomonas aeruginosa were greater than 20 mg L<sup>-1</sup> (Tappe et al., 2008), complicating efforts to identify environmentally-relevant MIC or IC<sub>50</sub> values for those antibiotic-bacteria pairs. As noted above, the broth microdilution assay is being increasingly applied to monitor residual antimicrobial activity and confirm formation of antimicrobially-active transformation products in wastewater (Szabó et al., 2017; Keen and Linden, 2013); however, it is important to note that other substances in wastewater may also contribute antimicrobial activity or interact with antibiotics and reduce their ability to enter cells or bind to biological targets. Many previous studies have employed Escherichia coli as a model organism (Wammer et al., 2006; Dodd et al., 2009); however, the aggregate data in Table S1 of the SI suggest opportunities to improve the sensitivity of residual antimicrobial activity analysis through selection of bacteria that are more susceptible to certain classes of antibiotics.

The objectives of this study were as follows: (1) elucidate the improved accuracy and precision of the  $IC_{50}$  parameter over the MIC for assessment of antimicrobial activity; (2) calculate the IC50 values of 13 bacteriostatic antibiotics from four environmentally-relevant classes (i. e., fluoroquinolones, macrolides, sulfonamides, and tetracyclines) for three bacteria (i.e., E. coli, Mycoplasma microti, and Pseudomonas fluorescens); and, (3) determine the optimal antibiotic-bacteria pairs for high-sensitivity analysis of antimicrobial activity. The principal outcomes of these objectives will improve the accuracy, precision, and sensitivity of protocols for measurement of antimicrobial activity associated with antibiotics of environmental concern. In fact, the four antibiotic classes were selected due to their incomplete removal during water and wastewater treatment and pseudo-persistence in the environment (Hopanna et al., 2020; He et al., 2015). Based on existing MIC literature (Table S1 in the SI), the E. coli, M. microti, and P. fluorescens bacteria species were hypothesized to demonstrate highly sensitive

analysis of growth inhibition (i.e., low  $IC_{50}$  values) for the antibiotics of concern. Multiple antibiotics were investigated from each class to identify the impacts of structural variations on the measured dose-response relationships with *E. coli, M. microti*, and *P. fluorescens*. Overall, the outcomes of this work are intended to provide a framework for bacteria selection to improve the sensitivity of antimicrobial activity assays, thereby enabling assessment of residual antimicrobial activity at concentrations more representative of those observed in environmental systems.

# 2. Materials and methods

#### 2.1. Chemicals and growth media

The investigated antibiotics were purchased in the following forms: ciprofloxacin (CIP); chlortetracycline (CTC) hydrochloride; clarithromycin (CLA); difloxacin (DIF) hydrochloride; enrofloxacin (ENR); erythromycin (ERY); oxytetracycline (OTC) dihydrate; sulfadiazine (SDZ); sulfacetamide (SAM) sodium salt monohydrate; sulfamerazine (SMR); sulfamethazine (SMZ) sodium salt; sulfamethoxazole (SMX) sodium salt; and, tylosin (TYL) tartrate. The chemical structures for the 13 antibiotics of concern are shown in Fig. S1 of the SI. Antibiotic standards were purchased from Sigma-Aldrich (St. Louis, MO, USA) or Fisher Scientific (Pittsburgh, PA, USA) at a purity of at least 98%. Antibiotic stock solutions were generated at 400 or 1000 mg L<sup>-1</sup> in deionized water (i.e., CTC, ERY, OTC, SAM, SMX, SMZ), deionized water with 12 mM NaOH (i.e., SDZ, SMR), or methanol (i.e., CIP, CLA, DIF, ENR, TYL) and stored at  $-20\,^{\circ}$ C. The addition of 12 mM NaOH and the use of methanol in some stock solutions stemmed from solubility constraints for particular antibiotics (Pomati et al., 2008). Working solutions with antibiotic concentrations ranging from 800  $\mu g L^{-1}$  to 1000 mg  $L^{-1}$  were prepared on a weekly basis by diluting stock solutions with deionized water or transferring an aliquot of the stock solutions to a separate container. Between uses, the working solutions were stored in the dark at 4  $^{\circ}$ C.

To reconstitute bacteria cultures and prepare inocula for antimicrobial activity assays, various media were required. Every month, phosphate buffered saline (PBS) was prepared at 10 mM and pH 7.2 and stored at 4 °C. Iso-sensitest broth (ISB) and agar (ISA) were prepared according to the manufacturer (Oxoid Limited; Hampshire, United Kingdom). Iso-sensitest media were used for all assays to maintain consistency in bacteria-to-bacteria comparisons and avoid interferences related to specific antibiotic mechanisms (Wammer et al., 2006; Hain et al., 2018). ISA and ISB are well-defined media, and the compositions are provided in Table S3 of the SI. ISA, ISB, and PBS were sterilized by autoclave at 121 °C and 15 psi for 15 min. Using CLSI guidelines, cell concentrations were calibrated to the optical density at 625 nm (OD625) using a McFarland 0.5 turbidity standard (equivalent to  $1-2 \times 10^8$  CFU mL $^{-1}$ ), which was prepared by mixing 1% barium chloride and 1% sulfuric acid at a ratio of 1:199 (CLSI, 2016).

# 2.2. Bacterial cultures

The following freeze-dried bacteria cultures were procured from the American Type Culture Collection (ATCC; Manassas, VA, USA): *E. coli* (ATCC 25922); *M. microti* (ATCC 700935); and, *P. fluorescens* (ATCC 21637). These three gram-negative bacteria were chosen based on their potential for sensitive analysis of the antibiotics of concern, as determined from the MIC values in Table S1 of the SI. The ATCC bacterial isolates were reconstituted in ISB, and then spread onto ISA plates using sterile sample loops. The plates were sealed with Parafilm to prevent contamination and evaporative losses. *E. coli* and *M. microti* were cultured at  $37 \pm 1$  °C for 16 h (CLSI, 2016; Brown et al., 2001), while *P. fluorescens* were grown in a separate incubator at  $26 \pm 2$  °C for 20 h. Individual colonies from each plate were collected using a sterile sample loop and deposited into separate 250-mL Erlenmeyer flasks containing 150 mL of ISB. The flasks were covered with Parafilm and incubated at

the conditions indicated above for 1–3 d (bacteria specific) to generate cultures with OD<sub>625</sub> values of approximately 2. The cultures were then mixed 1:1 (v/v) with 50% glycerol and deposited into 2-mL cryovials for storage at  $-80\,^{\circ}\mathrm{C}$  as bacterial seeds. Before experimentation, the *E. coli*, *M. microti*, and *P. fluorescens* seeds were thawed and diluted 1:100 (v/v) in ISB. These working cultures were incubated for 20–24 h at 37  $\pm$  1  $^{\circ}\mathrm{C}$  and 140 rpm for *E. coli* and *M. microti* and 26  $\pm$  2  $^{\circ}\mathrm{C}$  and 200 rpm for *P. fluorescens* before use in the antimicrobial activity assay.

# 2.3. Antimicrobial activity assay

The antimicrobial activity of antibiotics was measured as growth inhibition of *E. coli*, *M. microti*, and *P. fluorescens*. The assay protocol was adapted from the standard broth microdilution method (CLSI, 2016). For *E. coli* and *M. microti*, the assay was conducted in sterile, polystyrene 96-well plates (Corning Incorporated; Kennebunk, ME, USA). Sterile, black, glass-bottom 96-well plates (Greiner Bio-One; Kremsmünster, Austria) were used to accurately measure the optical density of *P. fluorescens* and the fluorescence of the pyoverdine siderophore produced by these bacteria (Scales et al., 2014). To measure growth inhibition as a function of antibiotic concentration, bacterial inocula were added to microplate wells containing serially-diluted antibiotic solutions. The plate design is shown in Fig. S2 of the SI and described below.

The serial dilution factor and initial antibiotic concentration were varied from CLSI guidelines (CLSI, 2016) to improve the resolution of the dose-response relationship for select antibiotics (Hacek et al., 1999). In particular, dilution factors of 1.5  $\times$  and 2  $\times$  were used. For the 1.5  $\times$ serial dilution, 100 µL of PBS was added to every well except A4-D4. Wells A4-D4 were filled with 300 µL of a solution containing 0.5-500  $mg L^{-1}$  of a particular antibiotic, and the first serial dilution was prepared by pipetting 200  $\mu L$  from wells A4-D4 to wells A5-D5 (which already contained 100  $\mu L$  of PBS). The mixtures in wells A5-D5 were aspirated four times by pipet, and then 200 µL was transferred to wells A6-D6. The serial dilution process continued to wells A12-D12, and the solutions in those wells were similarly diluted into wells E1-H1. Serial dilution continued in the same manner to wells E9-H9, wherein 200 μL was discarded after the aspiration step. For the 2  $\times$  serial dilution, the plate design was similar, except 100 µL of PBS was placed in every well, including wells A4-D4. Next,  $100~\mu L$  of a solution containing  $400{\text -}1000$  ${\rm mg}\,{\rm L}^{-1}$  of antibiotic was added to wells A4-D4, aspirated four times, and then  $100 \, \mu L$  was transferred during the serial dilution steps. The above protocols yielded 18 quadruplicate wells containing 100-µL solutions with antibiotic concentrations as low as 0.25  $\mu$ g L<sup>-1</sup> (for 1.5 × dilution) and 0.76  $\mu$ g L<sup>-1</sup> (for 2 × dilution) after addition of 100  $\mu$ L of the bacterial inoculum. Negative growth controls were generated in wells A1-D3 by adding 100 µL of ISB to 100 µL of PBS. Positive growth controls were placed in wells E10-H12 by adding 100 µL of inoculum to 100 µL of PBS. The total volume in the negative growth control, experimental, and positive growth control wells was 200 µL.

To generate the bacterial inocula, the working cultures described in Section 2.2 were diluted with ISB to match the OD<sub>625</sub> of the McFarland 0.5 turbidity standard. Optical density was measured with a Biotek Eon Microplate Spectrophotometer (Winooski, VT, USA). For E. coli and *M. microti*, this mixture was further diluted 100 × with ISB to achieve a cell concentration of  $1-2 \times 10^6$  CFU mL $^{-1}$ . These solutions were used as the bacterial inocula for microplates, with 100-µL aliquots being added to experimental and positive growth control wells (i.e., A4-D12, E1-H12). In accordance with CLSI recommendations, the cell concentration in each well was  $5-10 \times 10^5$  CFU mL<sup>-1</sup> (CLSI, 2016). For *P. fluorescens*, similar protocols were followed, but the final cell concentration in the experimental and positive growth control wells was 5  $\times$  10 $^{7}$  CFU mL $^{-1}$ to promote consistent P. fluorescens growth and pyoverdine production within the 16-20 h incubation period. The plates were sealed with Breathe-Easy oxygen permeable tape (Diversified Biotech; Dedham, MA, USA) and incubated for 16–20 h at 37  $\pm$  1  $^{\circ}$ C and 140 rpm for *E. coli* and M. microti and 26  $\pm$  2 °C and 200 rpm for P. fluorescens.

After the incubation period, the microplates were subjected to orbital mixing for 30 s to resuspend cells before  $OD_{625}$  measurement. The  $OD_{625}$  measurements were converted to growth inhibition using Eq. (1).

$$I_{OD} = \left(\frac{OD_{625,pos} - OD_{625,exp}}{OD_{625,pos} - OD_{625,neg}}\right) 100\% \tag{1}$$

In Eq. (1),  $I_{\rm OD}$  is the percent growth inhibition, and the 'pos', 'neg', and 'exp' labels indicate the positive growth control, negative growth control, and experimental samples, respectively.

To eliminate potentially confounding effects of the residual methanol content from the stock solutions of select antibiotics, separate doseresponse assays were run with variable methanol concentrations and no antibiotic. Based on the results (Fig. S3 in the SI), any experimental solutions with more than 1.0% methanol were excluded from the data analysis due to methanol-related impacts on bacterial growth. Based on the magnitude of measured IC50 values, this decision only affected microplate wells containing clarithromycin and tylosin concentrations greater than 125 mg  $\rm L^{-1}$ . The PBS content in experimental wells did not influence bacteria growth.

In accordance with visual assessment and previous protocols (CLSI, 2016; Hain et al., 2018), the lowest antibiotic concentration that resulted in an  $\rm I_{OD}$  greater than 80% was designated as the MIC. For example, if 40 mg  $\rm L^{-1}$  and 20 mg  $\rm L^{-1}$  antibiotic solutions caused 82% and 75% growth inhibition, respectively, the MIC was reported as 40 mg  $\rm L^{-1}$ . However, the 'true' MIC value would be in the 20–40 mg  $\rm L^{-1}$  range. To better capture this uncertainty, the MIC 'range' was reported as the highest antibiotic concentration with an  $\rm I_{OD}$  less than 80% to the lowest antibiotic concentration with an  $\rm I_{OD}$  greater than 80% (*i.e.*, 20–40 mg  $\rm L^{-1}$  for the above example).

For microplates containing *P. fluorescens*, 30 s of orbital mixing was employed before fluorescence measurement at excitation and emission wavelengths of 405 nm and 430 nm, respectively, using the Biotek Synergy H1 Multi-Mode Reader. These wavelengths correspond to pyoverdine and were confirmed by offline analyses (Fig. S4 in the SI) (Meyer, 2000; Wasserman, 1965; Dao et al., 1999). The potential overlap in antibiotic and pyoverdine fluorescence was assessed, but no interferences were observed (Fig. S4 in the SI). Fluorescence inhibition was, therefore, attributed to suppressed pyoverdine production; below, these responses will be referred to as pyoverdine inhibition, which was calculated using Eq. (2).

$$I_{FL} = \left(\frac{FL_{pos} - FL_{exp}}{FL_{pos} - FL_{neg}}\right) 100\% \tag{2}$$

In Eq. (2),  $I_{FL}$  is the percent pyoverdine inhibition, FL is the fluorescence intensity for excitation at 405 nm and emission at 430 nm, and the 'pos', 'neg', and 'exp' labels are the same as in Eq. (1).

All optical density and fluorescence measurements were recorded in triplicate, and the mean values were used for analysis; note, the relative standard deviation was always less than 5%. The quadruplicate experimental  $I_{OD}$  and  $I_{FL}$  data were fit to the Hill equations shown in Eq. (3) and Eq. (4), respectively. The models were fit with OriginPro 9.3 (Northampton, MA, USA) to obtain the Hill parameters (e.g.,  $I_{OD,max}$ ,  $I_{OD,min}$ ,  $I_{C50}$ , and  $I_{C50}$ 

$$I_{\text{OD}} = \begin{bmatrix} I_{\text{OD,max}} - I_{\text{OD,min}} \\ 1 + \left(\frac{I_{\text{Cs}_0}}{C}\right)^{\text{H}_{\text{OD}}} + I_{\text{OD,min}} \end{bmatrix} 100\%$$
 (3)

$$I_{FL} = \begin{bmatrix} I_{FL,max} - I_{FL,min} \\ 1 + \left(\frac{EC_{50}}{C}\right)^{H_{FL}} + & I_{FL,min} \end{bmatrix} \quad 100\%$$
 (4)

In Eqs. (3)–(4), the 'max' and 'min' labels indicate the maximum and minimum percent inhibition, respectively,  $IC_{50}$  is the antibiotic concentration that causes 50% growth inhibition, C is the antibiotic concentration in the well,  $H_{OD}$  is the Hill slope for optical density measurements,  $EC_{50}$  is the antibiotic concentration that causes 50% pyoverdine inhibition, and  $H_{FL}$  is the Hill slope for fluorescence measurements.

# 3. Results and discussion

#### 3.1. Comparison of MIC and IC50 values

Previous work has mostly described antimicrobial activity in terms of the MIC value, as suggested by the data in Table S1 of the SI (Wei et al., 2019; Catania et al., 2019; Wetzstein, 2005; Linde et al., 2000; Winissorn et al., 2013; Mouneimné et al., 1999; Voigt et al., 2019; de Boer et al., 2015; Heuvelink et al., 2016; Felde et al., 2018; Peng et al., 2014; Voigt et al., 2018; Voigt et al., 2017; Mizdal et al., 2018). For environmental analysis, antimicrobial activity metrics should have high accuracy, precision, and sensitivity (i.e., low MIC values). Using the standard CLSI protocol, the potential values that can be recorded for the MIC are experimentally constrained by the highest antibiotic concentration and the serial dilution factor (Hain et al., 2018). In particular, the broth

microdilution protocol suggests an initial antibiotic concentration of 256 mg  $L^{-1}$  and 12 serial dilutions (dilution factor =2) to 0.125 mg  $L^{-1}$  (CLSI, 2016). This protocol complicates identification of the true MIC and lowers the accuracy of the MIC parameter. For a 2  $\times$  dilution factor, the uncertainty on the MIC is 50%, and the magnitude of the uncertainty increases for higher MIC values. Consider the difference between 256 and 128 mg  $L^{-1}$ , compared to 0.250 and 0.125 mg  $L^{-1}$ . On the contrary, the uncertainty of the IC50 parameter can be minimized through the use of replicates and curve fitting.

The observed MIC ranges and  $IC_{50}$  values for the antibiotic-bacteria pairs are reported in Table 1. For the  $IC_{50}$  data, the median 95% confidence interval was 8.9% of the  $IC_{50}$  value, indicating better precision than the MIC. The MIC values and ranges were plotted against the  $IC_{50}$  parameters for all antibiotic-bacteria pairs in Fig. 1. The magnitude of the MIC was always greater than that of the  $IC_{50}$ , highlighting the better sensitivity of the  $IC_{50}$  parameter. Several MIC values were considerably higher than the corresponding  $IC_{50}$  parameters (e.g., clarithromycin against *M. microti*). These MICs generally stemmed from models with lower  $I_{OD,max}$  parameters, which were more common for *E. coli*. These findings, coupled to the high potential for personal (e.g., visual inspection) and systematic (e.g., impacts of initial concentration and dilution factor) bias, indicate that  $IC_{50}$  values are better suited to environmental applications of antimicrobial activity assays. From a practical perspective, the  $IC_{50}$  can be utilized in similar manners as other acute toxicity

**Table 1**Hill equation parameters and MIC values for growth inhibition of *E. coli. M. microti.* and *P. fluorescens* by the antibiotics of concern.

Class	Antibiotic	Organism	$IC_{50} (mg L^{-1})^a$	$H_{OD}^{a}$	I <sub>OD,min</sub> (%) <sup>a</sup>	I <sub>OD,max</sub> (%) <sup>a</sup>	MIC range (mg $L^{-1}$ ) $^{b}$
Fluoroquinolone	Ciprofloxacin	E. coli	$0.0034 \pm 0.0003$	$2.38 \pm 0.46$	$-1.42 \pm 4.66$	$87.7 \pm 2.0$	0.0087 - 0.0130
		M. microti	$0.041\pm0.002$	$7.63\pm1.59$	$\textbf{-8.36} \pm \textbf{1.87}$	$100.1\pm2.8$	0.0351 - 0.0527
		P. fluorescens	$0.016\pm0.001$	$3.54 \pm 0.41$	$\textbf{-2.19} \pm 1.53$	$95.5\pm1.5$	0.0195 - 0.0293
	Difloxacin	E. coli	$0.0051 \pm 0.0002$	$5.59 \pm 0.79$	$1.15\pm1.69$	$100.0\pm1.5$	0.0065 - 0.0098
		M. microti	$0.083\pm0.012$	$2.97 \pm 1.11$	$7.36 \pm 3.68$	$106.7 \pm 9.8$	0.079 - 0.119
		P. fluorescens	$0.034 \pm 0.008$	$1.29 \pm 0.35$	$3.57 \pm 8.74$	$100.6 \pm 4.5$	0.098 - 0.146
	Enrofloxacin	E. coli	$0.0066 \pm 0.0003$	$3.95\pm0.68$	$1.14 \pm 2.28$	$87.3\pm1.6$	0.0195 - 0.0293
		M. microti	$0.073\pm0.004$	$5.82 \pm 1.49$	$\textbf{4.42} \pm \textbf{2.04}$	$107.2\pm3.9$	0.079 - 0.119
		P. fluorescens	$0.125\pm0.005$	$6.65\pm1.13$	$-7.93 \pm 1.49$	$96.5 \pm 3.3$	0.148 - 0.222
Macrolide	Clarithromycin	E. coli	$17.9 \pm 4.8$	$1.87 \pm 0.79$	$9.65 \pm 5.32$	$104.0\pm13.7$	32.9 - 49.4
	•	M. microti	$0.051 \pm 0.008$	$3.67\pm1.85$	$\textbf{-13.7} \pm \textbf{6.9}$	$84.3 \pm 4.1$	1.95 – 3.91
		P. fluorescens	$48.1 \pm 4.3$	$2.37 \pm 0.47$	$2.60\pm2.54$	98.4 <sup>c</sup>	<i>74.1</i> – 111.1
	Erythromycin	E. coli	$13.8 \pm 2.3$	$0.97 \pm 0.16$	$8.04 \pm 3.87$	$105.1 \pm 5.5$	21.9 - 32.9
	, ,	M. microti	$1.60\pm0.59$	$1.00\pm0.33$	$\textbf{-12.2} \pm 7.0$	$106.3 \pm 9.4$	1.95 - 3.91
		P. fluorescens	$67.7 \pm 4.4$	$0.92 \pm 0.06$	$\textbf{-6.08} \pm 1.50$	100 <sup>c</sup>	167 – 250
	Tylosin	E. coli	$23.3 \pm 2.9$	$1.85 \pm 0.31$	$\textbf{-0.07} \pm 1.38$	$110.0 \pm 7.9$	25 - 50
	·	M. microti	$0.032\pm0.007$	$2.07 \pm 0.86$	$3.19 \pm 8.69$	$100.6 \pm 5.1$	0.061 - 0.122
		P. fluorescens	$22.1\pm1.6$	$3.82\pm1.04$	$\textbf{-3.41} \pm 1.78$	$99.3 \pm 5.4$	25 - 50
Sulfonamide	Sulfacetamide	E. coli	$13.8\pm1.5$	$7.13 \pm 6.60$	$6.03 \pm 5.02$	$98.5 \pm 8.5$	13.2 – 19.8
		M. microti	$8.98 \pm 0.92$	$3.73\pm1.32$	$1.43 \pm 2.51$	$98.1 \pm 4.4$	7.8 – 15.6
		P. fluorescens	$12.8\pm1.6$	$\textbf{7.32} \pm \textbf{2.01}$	$-6.54 \pm 1.60$	$97.1 \pm 2.6$	13.2 – 19.8
	Sulfadiazine	E. coli	$4.76\pm0.23$	$2.51\pm0.27$	$\textbf{-1.13} \pm \textbf{1.24}$	$97.0\pm1.9$	13.2 – 19.8
		M. microti	$2.58 \pm 0.30$	$4.20\pm1.40$	$4.59 \pm 2.87$	$95.5 \pm 3.7$	1.95 - 3.91
		P. fluorescens	$19.1 \pm 3.8$	$1.94 \pm 0.61$	$3.65 \pm 2.35$	$64.9 \pm 6.6$	$> 100^{\rm d}$
	Sulfamerazine	E. coli	$19.4\pm1.3$	$2.35 \pm 0.30$	$\textbf{-0.66} \pm 1.05$	$91.8 \pm 2.7$	<i>50</i> – 100
		M. microti	$2.48 \pm 0.17$	$4.07 \pm 0.85$	$\textbf{-1.15} \pm \textbf{1.87}$	$97.4 \pm 2.4$	1.95 - 3.91
		P. fluorescens	$> 100^{d}$	_e	_e	_e	$> 100^{\rm d}$
	Sulfamethazine	E. coli	$9.63\pm1.48$	$2.22\pm0.65$	$\textbf{-1.09} \pm \textbf{2.41}$	$83.3 \pm 4.9$	25 - 50
		M. microti	$4.19 \pm 0.21$	$3.95 \pm 0.86$	$3.45\pm1.39$	$98.3 \pm 2.0$	3.91 - 7.81
		P. fluorescens	$> 100^{d}$	_e	_e	_e	> 100 <sup>d</sup>
	Sulfamethoxazole	E. coli	$15.1\pm1.3$	$5.85 \pm 2.35$	$12.5\pm2.9$	$98.2 \pm 5.3$	<i>13.2</i> – 19.8
		M. microti	$\textbf{0.814} \pm \textbf{0.108}$	$4.00\pm1.80$	$\textbf{-33.3} \pm 5.6$	$99.2 \pm 5.6$	0.98 - 1.95
		P. fluorescens	$11.2 \pm 0.5$	$4.64 \pm 0.74$	$\textbf{7.04} \pm \textbf{1.42}$	$97.5 \pm 2.3$	<i>13.2</i> – 19.8
Tetracycline	Chlortetracycline	E. coli	$0.318 \pm 0.018$	$2.26\pm0.25$	$\textbf{-0.54} \pm 1.47$	$104.9\pm1.5$	0.391 - 0.781
	•	M. microti	$64.1\pm12.5$	$5.5\pm12.6$	$\textbf{-11.9} \pm \textbf{6.4}$	$99.9 \pm 21.8$	<i>62.5</i> – 125.0
		P. fluorescens	$0.119 \pm 0.006$	$4.85 \pm 0.93$	$1.82\pm1.63$	$97.8 \pm 1.4$	0.098 - 0.195
	Oxytetracycline	E. coli	$0.139 \pm 0.014$	$2.78 \pm 0.70$	$5.30 \pm 4.81$	$99.9 \pm 3.0$	0.145 - 0.217
		M. microti	$1.96\pm0.09$	$6.13 \pm 5.25$	$\textbf{2.74} \pm \textbf{2.11}$	$99.4 \pm 2.6$	1.95 - 3.91
		P. fluorescens	$0.245\pm0.022$	$2.93\pm0.66$	$-3.62\pm3.91$	$99.6 \pm 3.2$	0.325 - 0.488

 $<sup>^{</sup>m a}$  Mean value  $\pm$  95% confidence interval.

b The italicized value is the lower end of the MIC range (i.e., MIC divided by dilution factor) and the second value is the observed MIC.

<sup>&</sup>lt;sup>c</sup> I<sub>OD,max</sub> was fixed due to a low number of data points at high growth inhibition.

 $<sup>^{</sup>m d}$  The IC $_{
m 50}$  or MIC value was greater than the highest tested antibiotic concentration.

<sup>&</sup>lt;sup>e</sup> The Hill equation could not be fit due to the low growth inhibition observed for the tested antibiotic concentrations.

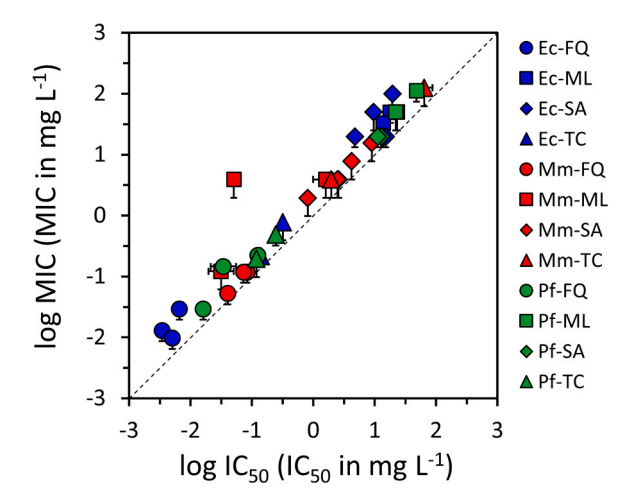


Fig. 1. The MIC values and ranges (in log units) plotted against the  $IC_{50}$  parameters (in log units) for all antibiotic-bacteria pairs. The symbols are located at the observed MIC values (y-axis) and mean  $IC_{50}$  parameters (x-axis) from quadruplicate measurements. The error bars in the y-direction represent the MIC range, stemming from the observed MIC (symbol) to the observed MIC divided by the dilution factor (bottom of the error bar). The error bars in the x-direction are 95% confidence intervals on the  $IC_{50}$ . The symbol shapes and colors are defined in the legend, where 'Ec', 'Mm', and 'Pf' indicate *E. coli*, *M. microti*, and *P. fluorescens*, respectively, and 'FQ', 'ML', 'SA', and 'TC' represent fluoroquinolone, macrolide, sulfonamide, and tetracycline antibiotics, respectively.

parameters, such as the half-maximal lethal concentration ( $LC_{50}$ ) used to describe toxic outcomes in higher organisms.

# 3.2. Bacteria-specific antibiotic activity

The IC<sub>50</sub> and EC<sub>50</sub> parameters are reported for all antibiotic-bacteria pairs in Table 1 and Table 2, respectively. The most potent antibiotics from each class were identified as those with the lowest IC<sub>50</sub> or EC<sub>50</sub> values: ciprofloxacin (fluoroquinolone) inhibition of *E. coli* growth (IC<sub>50</sub> = 3.4  $\pm$  0.3  $\mu g$  L $^{-1}$ ); tylosin (macrolide) inhibition of *M. microti* growth (IC<sub>50</sub> = 32  $\pm$  7  $\mu g$  L $^{-1}$ ); sulfamethoxazole (sulfonamide) inhibition of *M. microti* growth (IC<sub>50</sub> = 814  $\pm$  108  $\mu g$  L $^{-1}$ ); and, chlortetracycline (tetracycline) inhibition of *P. fluorescens* growth (IC<sub>50</sub> = 119  $\pm$  6  $\mu g$  L $^{-1}$ ) and pyoverdine production (EC<sub>50</sub> = 107  $\pm$  10  $\mu g$  L $^{-1}$ ). The potency of these four antibiotics varied for the other microorganisms. For example, the IC<sub>50</sub> values for chlortetracycline growth inhibition of *E. coli* and *M. microti* were 2.7  $\times$  and 539  $\times$  the *P. fluorescens* IC<sub>50</sub>, respectively; similarly, the IC<sub>50</sub> values for tylosin growth inhibition of *E. coli* and *P. fluorescens* were 728  $\times$  and 691  $\times$  the *M. microti* IC<sub>50</sub>, respectively.

These findings highlight the variable efficacy of antibiotic mechanisms of action for different microorganisms. For the above example, chlortetracycline binding to the 30S ribosomal subunit (Chukwudi, 2016) effectively inhibited the growth of *P. fluorescens* but not that of *M. microti*, which was more sensitive to tylosin interactions at the 50S ribosomal subunit (Kannan et al., 2014). The differences in antimicrobial activity stem from structural variations in the inhibited proteins or rRNA (Melnikov et al., 2018), although it should be noted that the mechanisms of action for some antibiotic classes are not fully understood (Chukwudi, 2016; Kannan et al., 2014). Importantly, the 1–3 order of magnitude variation in IC<sub>50</sub> values for antibiotics with different microorganisms reinforced opportunities to improve the sensitivity of residual antimicrobial activity assays for environmental applications through more deliberate bacteria selection practices.

Despite the variable effects of antibiotics on growth inhibition of the three bacteria (Table 1), fluoroquinolones were generally more potent than macrolides, sulfonamides, and tetracyclines. For example, tylosin was the most potent macrolide for *P. fluorescens* (IC $_{50}=22.1\pm1.6~\text{mg L}^{-1}$ ), but ciprofloxacin was almost  $1400\times\text{more}$  potent (IC $_{50}=16\pm1~\mu\text{g L}^{-1}$ ). Over the last 80 years, the development of new antibiotics has focused on chemical substitutions at the baseline pharmacophore of each antibiotic class to enhance inhibition of essential cellular processes (Maguna et al., 2016). For this reason, the antimicrobial potency of antibiotics also varies within each class. The following subsections discuss specific results for fluoroquinolone, macrolide, sulfonamide, and tetracycline antibiotics.

#### 3.2.1. Antimicrobial activity of fluoroquinolones

The data in Table 1 indicated that the three fluoroguinolone antibiotics were relatively effective against E. coli, M. microti, and P. fluorescens. In fact, the highest  $IC_{50}$  was only 125  $\mu g L^{-1}$ , which is the lowest concentration assayed in the conventional CLSI protocol (CLSI, 2016), confirming the need for optimization of these protocols for environmental analyses. As an example, Fig. 2 shows the difloxacin dose-response curves for growth inhibition of E. coli (IC50  $= 5.1 \pm 0.2 \ \mu g \ L^{-1}), \quad M. \quad \textit{microti} \quad (IC_{50} = 83 \pm 12 \ \mu g \ L^{-1}), \quad \text{and}$ *P.* fluorescens (IC<sub>50</sub> =  $34 \pm 8 \mu g L^{-1}$ ). Pyoverdine inhibition in P. fluorescens occurred at lower difloxacin concentrations (EC<sub>50</sub>  $=23\pm10~\mu g~L^{-1}$ ) than growth inhibition, and this trend held for all of the investigated antibiotics (see Table 2 and Section 3.3 for more discussion of pyoverdine inhibition). These results highlighted the potential advantages of using sublethal effects, such as pyoverdine inhibition, to monitor antibiotic activity, although the advantage was minor for difloxacin and other fluoroquinolones.

The observed MIC range (8.7–13.0  $\mu g \, L^{-1}$ ) of ciprofloxacin for growth inhibition of *E. coli* aligned with previously reported MIC values (6–15  $\mu g \, L^{-1}$ ) (Wetzstein, 2005; Linde et al., 2000; Winissorn et al., 2013). Furthermore, the measured IC<sub>50</sub> (3.4  $\pm$  0.3  $\mu g \, L^{-1}$ ) was slightly

**Table 2**Hill equation parameters for pyoverdine inhibition in *P. fluorescens* by the fluoroquinolone, macrolide, sulfonamide, and tetracycline antibiotics.

Class	Antibiotic	$EC_{50} (mg L^{-1})^{a}$	$H_{\mathrm{FL}}^{}a}$	$I_{FL,min}$ (%) <sup>a</sup>	$I_{FL,max}$ (%) <sup>a</sup>
Fluoroquinolone	Ciprofloxacin	$0.010 \pm 0.001$	$2.62 \pm 0.38$	$-5.42\pm2.72$	$99.0 \pm 2.2$
	Difloxacin	$0.023\pm0.010$	$1.68\pm1.03$	$11.6\pm17.8$	$101.1 \pm 7.6$
	Enrofloxacin	$0.102\pm0.009$	$10.3\pm17.3$	$17.0\pm3.4$	$98.3 \pm 6.8$
Macrolide	Clarithromycin	$26.6\pm1.9$	$1.43\pm0.03$	$-15.7\pm2.5$	$100.2^{b}$
	Erythromycin	$41.9 \pm 5.1$	$3.52\pm1.30$	$-9.45 \pm 4.07$	$99.6 \pm 8.5$
	Tylosin	$12.0\pm2.8$	$2.43\pm1.20$	$-1.77 \pm 4.48$	$105.5\pm12.5$
Sulfonamide	Sulfacetamide	$4.32 \pm 0.96$	$0.96 \pm 0.22$	$0.26 \pm 6.43$	$108.1 \pm 7.6$
	Sulfadiazine	$6.19 \pm 2.06$	$0.99 \pm 0.33$	$-19.5 \pm 9.9$	$114.0 \pm 15.4$
	Sulfamerazine	$31.6 \pm 6.0$	$1.08 \pm 0.24$	$-0.66\pm1.05$	$100^{\mathrm{b}}$
	Sulfamethazine	$49.6 \pm 25.7$	$0.49 \pm 0.20$	$-1.55\pm1.87$	$100^{\mathrm{b}}$
	Sulfamethoxazole	$1.55 \pm 0.39$	$1.18 \pm 0.33$	$-1.5\pm10.1$	$103.6 \pm 5.6$
Tetracycline	Chlortetracycline	$0.107\pm0.010$	$3.71\pm1.25$	$2.95 \pm 3.17$	$100.7\pm2.7$
	Oxytetracycline	$0.133\pm0.014$	$\textbf{2.34} \pm \textbf{0.49}$	$-9.79 \pm 5.31$	$100.2 \pm 3.0$

<sup>&</sup>lt;sup>a</sup> Mean value  $\pm$  95% confidence interval.

b I<sub>Fl.max</sub> was fixed due to a low number of data points at high pyoverdine inhibition.

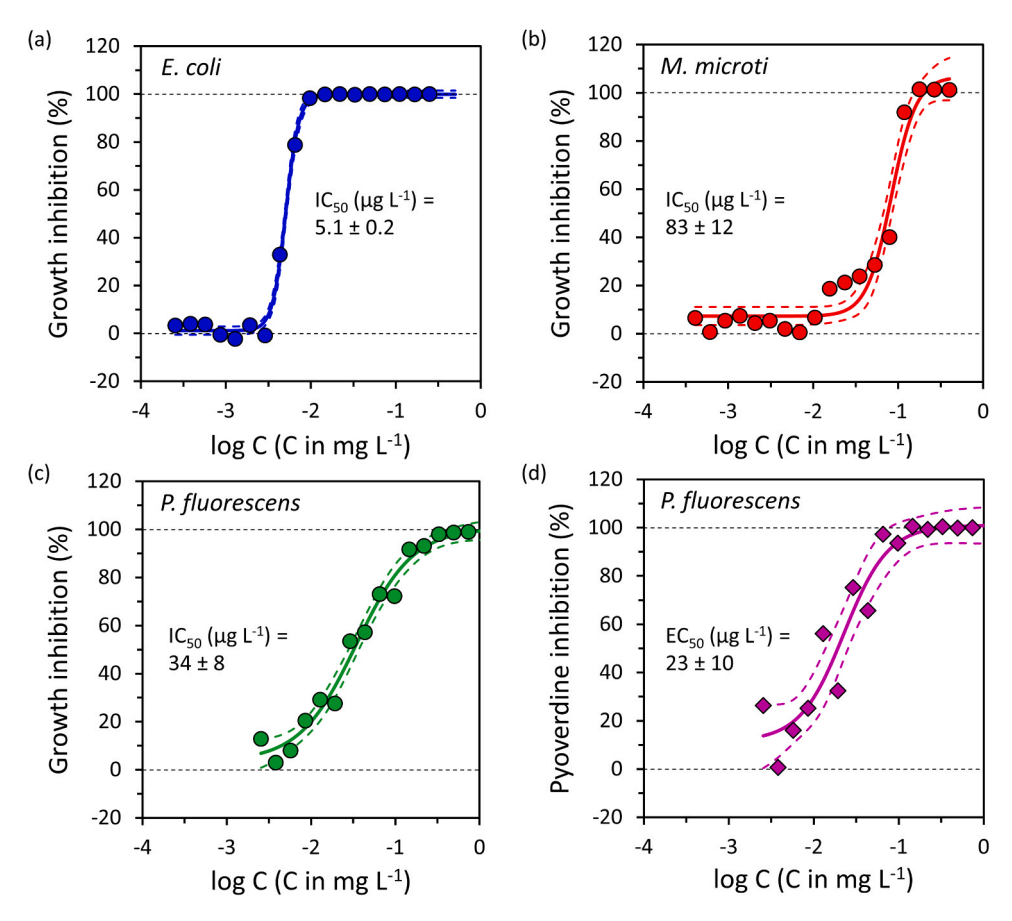


**Fig. 2.** Dose-response curves for difloxacin and (a) *E. coli* growth inhibition, (b) *M. microti* growth inhibition, and *P. fluorescens* (c) growth inhibition and (d) pyoverdine inhibition. The solid curves are the best fit Hill models, and the dashed curves are the 95% confidence bands. The symbols are the mean inhibition from quadruplicate measurements. The complete list of Hill equation model parameters is reported in Table 1 for growth inhibition and Table 2 for pyoverdine inhibition.

lower than the value (7.9  $\pm$  0.5  $\mu g$  L<sup>-1</sup>) determined by He et al. (2015), who employed similar protocols but used a different growth medium. The adjustments to the assay protocols also improved the sensitivity of P. fluorescens growth inhibition by ciprofloxacin; in particular, an IC<sub>50</sub> of  $16 \pm 1 \,\mu g \, L^{-1}$  was measured in this study, whereas previous efforts could not determine the IC  $_{50}$  and only reported an MIC of  $<100\ \mu g\ L^{-1}$ (Voigt et al., 2019). While no previous reports were identified for fluoroquinolone inhibition of M. microti, the observed MIC range of enrofloxacin (79–119  $\mu$ g L<sup>-1</sup>) was lower than previously reported MIC values for the related organisms, Mycoplasma bovis (250 µg L<sup>-1</sup>) (Heuvelink et al., 2016), Mycoplasma hyopneumoniae (312 µg L<sup>-1</sup>) (Felde et al., 2018), and Mycoplasma synoviae (> 16 mg  $L^{-1}$ ) (Catania et al., 2019). The IC<sub>50</sub> values of fluoroquinolones for *E. coli* were lower than those for M. microti and P. fluorescens; therefore, the E. coli model organism provided highly sensitive analysis of antimicrobial activity. The experimental data for individual fluoroquinolones provided additional insight to the impacts of chemical structure on antimicrobial activity.

The dose-response data indicated that fluoroquinolone functional group substitutions play an important role in antimicrobial activity. The ciprofloxacin IC $_{50}$  values for E. coli and M. microti were lower than those of difloxacin (50% and 102% higher, respectively) and enrofloxacin (94% and 78% higher, respectively) (Table 1). Similar results were found for ciprofloxacin (IC $_{50}=16\pm1~\mu g~L^{-1}$ ), difloxacin (IC $_{50}=34\pm8~\mu g~L^{-1}$ ), and enrofloxacin (IC $_{50}=125\pm5~\mu g~L^{-1}$ ) with P. fluorescens. The chemical structures of ciprofloxacin and enrofloxacin differ by the piperazinyl and ethylpiperazinyl groups, respectively, at C12 and C9 (Fig. S1 in the SI); furthermore, enrofloxacin and difloxacin differ by the cyclopropyl and fluorophenyl groups, respectively, at N18 and N15 and the ethylpiperazinyl and methylpiperazinyl groups, respectively, at C9 and C8. The IC $_{50}$  values of difloxacin for E. coli and

P. fluorescens were lower than those of enrofloxacin (29–268% higher; Table 1); however, the difloxacin and enrofloxacin IC50 values were similar for M. microti. In aggregate, these results established enrofloxacin as the least potent fluoroquinolone for E. coli and P. fluorescens, whereas difloxacin and enrofloxacin exhibited similarly low activity against M. microti. Contextualizing these results with those from ciprofloxacin (the most potent fluoroquinolone), the ethyl group on the piperazinyl ring in enrofloxacin reduced the antimicrobial activity for all organisms, in agreement with previous findings (Chu and Fernandes, 1989). The acid dissociation constants (Ka values) at N16, N2, and N3 are  $10^{-8.68}$ ,  $10^{-6.42}$ , and  $10^{-6.66}$  in ciprofloxacin, difloxacin, and enrofloxacin, respectively (Garg et al., 2007). Therefore, ciprofloxacin is more protonated than difloxacin and enrofloxacin in the growth medium (pH 7.2). The lower potency of difloxacin and enrofloxacin compared to ciprofloxacin may, therefore, stem from steric and/or electronic effects that reduce antibiotic (i) binding to DNA gyrase or topoisomerase IV or (ii) transport into the cell (Vergalli et al., 2017; Peterson, 2001). The cyclopropyl substitution at N6 (ciprofloxacin) and N18 (enrofloxacin) improved hydrophobic interactions with DNA and conferred stronger binding compared to difloxacin (Chu and Fernandes, 1989). In these ways, the structural variations between fluoroquinolone molecules were associated with observed differences in antimicrobial activity. These findings have important implications for application of antimicrobial activity assays for assessment of environmental transformation products of antibiotics.

# 3.2.2. Antimicrobial activity of macrolides

As indicated in Table 1, the macrolide antibiotics were most potent against *M. microti*, followed by *E. coli*, and then *P. fluorescens*. The doseresponse curves in Fig. 3 demonstrated that tylosin was almost three

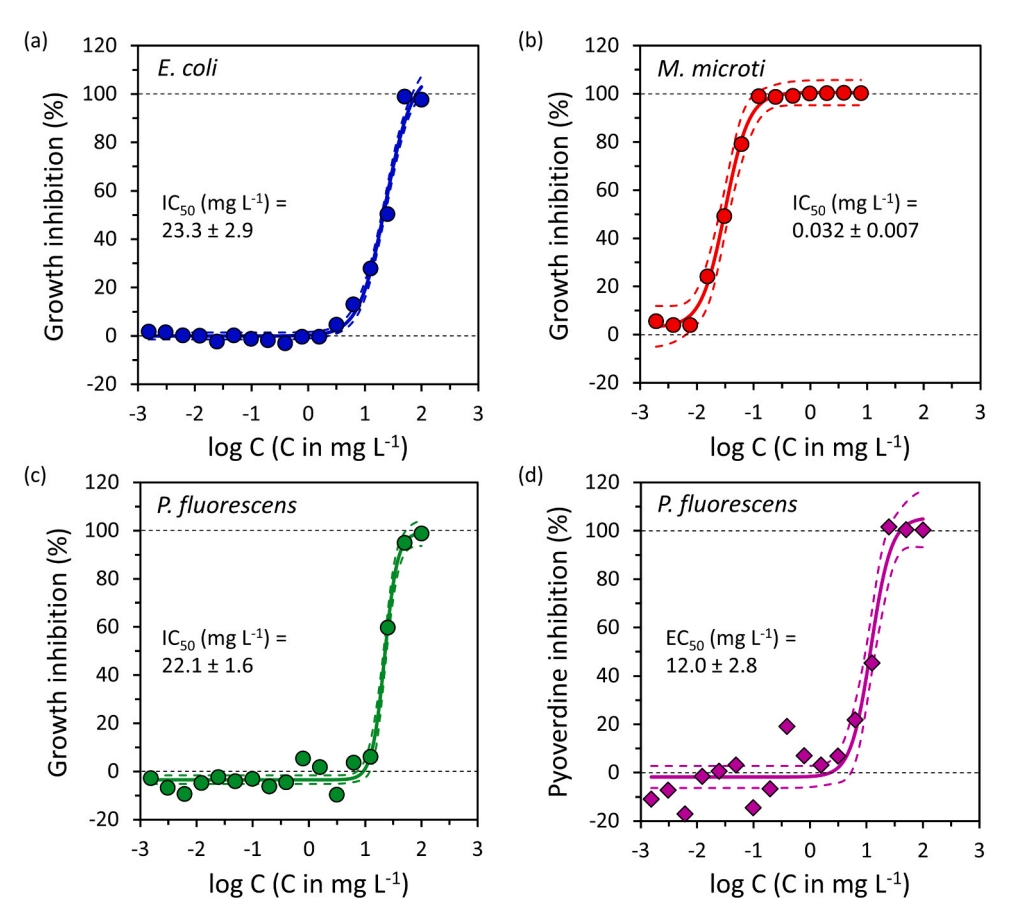


**Fig. 3.** Dose-response curves for tylosin and (a) *E. coli* growth inhibition, (b) *M. microti* growth inhibition, and *P. fluorescens* (c) growth inhibition and (d) pyoverdine inhibition. The solid curves are the best fit Hill models, and the dashed curves are the 95% confidence bands. The symbols are the mean inhibition from quadruplicate measurements. The complete list of Hill equation model parameters is reported in Table 1 for growth inhibition and Table 2 for pyoverdine inhibition.

orders of magnitude more potent against M. microti (IC<sub>50</sub> =  $32 \pm 7 \,\mu\text{g L}^{-1}$ ) compared to P. fluorescens (IC<sub>50</sub> =  $22.1 \pm 1.6 \,\text{mg L}^{-1}$ ) and E. coli (IC  $_{50}~=23.3\pm2.9~mg~L^{-1}).$  The IC  $_{50}~$  of tylosin for P. fluorescens was similar to the value (25.82  $\pm$  0.57 mg  $L^{-1}$ ) reported by Voigt et al. (2019). Furthermore, the MIC range (61–122  $\mu$ g L<sup>-1</sup>) of tylosin for M. microti overlapped with an MIC value reported for Mycoplasma synoviae (62.5  $\mu$ g L<sup>-1</sup>) (Catania et al., 2019) but was lower than MIC parameters for Mycoplasma hyopneumoniae (500  $\mu$ g L<sup>-1</sup>) (Felde et al., 2018) and Mycoplasma bovis (64 mg  $L^{-1}$ ) (Heuvelink et al., 2016). These data highlight the species-specific sensitivity of Mycoplasma spp. to macrolides. Tylosin (IC50 =  $22.1 \pm 1.6$  mg  $L^{-1}$ ) was more potent than clarithromycin (IC<sub>50</sub> =  $48.1 \pm 4.3$  mg L<sup>-1</sup>) and erythromycin (IC<sub>50</sub>  $=67.7\pm4.4$  mg  $L^{-1}$ ) for growth inhibition of P. fluorescens. This trend was conserved for pyoverdine inhibition (Table 2), suggesting that the structural differences between these three antibiotics exhibited notable effects on both lethal and sublethal activity. For E. coli, clarithromycin (IC  $_{50}~=17.9\pm4.8~\text{mg L}^{-1})~$  and ~ erythromycin (IC  $_{50}~=13.8\pm$ 2.3 mg  $L^{-1})$  were slightly more potent than tylosin (IC  $_{50}=23.3\pm$ 2.9 mg L<sup>-1</sup>). Clarithromycin and tylosin exhibited strong inhibitory effects on M. microti growth and were 1-2 orders of magnitude more potent than erythromycin. The aggregate dose-response data highlighted the opportunity to use a less-studied bacteria, namely M. microti, for sensitive analysis of the antimicrobial activity of macrolides.

The structural differences between the macrolide antibiotics were investigated to determine their effects on antimicrobial activity. The size of the lactone ring is the most notable structural difference between tylosin (16-atom ring) and clarithromycin and erythromycin (14-atom rings) (Fig. S1 in the SI); however, tylosin also has conjugated bonds and an additional substituted oxane ring that may affect antimicrobial activity. Macrolides inhibit protein synthesis by binding to the 50S

ribosomal subunit and other sites (Tenson et al., 2003). The macrolides with 14-atom rings block translocation of peptidyl-tRNA, whereas macrolides with 16-atom rings inhibit the peptidyl transfer reaction (Mazzei et al., 1993). These differences might account for the higher potency of tylosin for P. fluorescens, although no similar benefits were observed in E. coli or M. microti, suggesting bacteria-specific opportunities to improve the sensitivity of antimicrobial activity analysis. Clarithromycin was more potent than erythromycin for M. microti and P. fluorescens but not for E. coli. In general, the experimental data indicated that the order from most-to-least potent macrolide was tylosin, clarithromycin, and erythromycin. Erythromycin and tylosin are naturally-occurring antibiotics, but clarithromycin is a semisynthetic molecule derived from erythromycin (Mazzei et al., 1993). As noted above, the lactone ring of tylosin differs from that of clarithromycin and erythromycin. The only structural differences between clarithromycin and erythromycin are the methyl ether and hydroxyl groups, respectively, on C37 (Fig. S1 in the SI). The significant impact of these minor structural differences on antimicrobial potency may stem from the higher chemical and metabolic stability of clarithromycin (Mazzei et al., 1993), and such impacts may have important implications for environmental transformation products of macrolides.

# 3.2.3. Antimicrobial activity of sulfonamides

Based on the IC<sub>50</sub> parameters reported in Table 1, the sulfonamides were most potent against *M. microti*. A similar conclusion can be reached from Fig. S5 of the SI, which shows the dose-response curves of sulfamethoxazole for the three bacteria. The range of IC<sub>50</sub> values for sulfonamides against the *E. coli* model organism was relatively small, from  $4.76\pm0.23$  mg  $L^{-1}$  for sulfadiazine to  $19.4\pm1.3$  mg  $L^{-1}$  for sulfamerazine, suggesting minor impacts of substituted groups. The

sensitivity of the assay also varied with bacteria type. For example, sulfamethoxazole exhibited IC $_{50}$  values of  $15.1\pm1.3$ ,  $11.2\pm0.5$ , and  $0.814\pm0.108$  mg L $^{-1}$  against *E. coli*, *P. fluorescens*, and *M. microti*, respectively. In general, the measured IC $_{50}$  parameters for sulfonamides (Table 1) aligned with the previous reports compiled in Table S2 in the SI. For example, the IC $_{50}$  of sulfamethoxazole for *P. fluorescens* ( $11.2\pm0.5$  mg L $^{-1}$ ) was within the same order of magnitude as the  $3.90\pm0.11$  mg L $^{-1}$  value reported by Voigt et al. (2019), who used a different growth medium. Similarly, the measured IC $_{50}$  of sulfamethoxazole for *E. coli* ( $15.1\pm1.3$  mg L $^{-1}$ ) was slightly higher than that identified for a different *E. coli* strain ( $3.21\pm0.30$  mg L $^{-1}$ ) by Wammer et al. (2006), who used a shorter incubation time (8 h). Sulfamethazine and sulfamerazine were considered to be ineffective against *P. fluorescens* as none of the tested concentrations caused more than 50% growth inhibition, suggesting IC $_{50}$  values greater than 100 mg L $^{-1}$ .

No previous reports of sulfonamide inhibition of M. microti are available in the literature; however, the susceptibility of M. microti to sulfonamide antibiotics was unexpected as Mycoplasma spp. do not typically synthesize folic acid and are considered to be resistant to sulfonamides and trimethoprim (McCormack, 1993). Mycoplasma spp. generally grow in folate-rich environments (Arraes et al., 2007; de Crécy-Lagard et al., 2007; Chernova et al., 2016). In this case, M. microti may have obtained enough purine and pyrimidine nucleotides from the growth medium (Table S3 in the SI) to grow for the 16-20 h incubation period. This phenomenon would suggest that the experimental results stem from an alternative mechanism of action, such as inhibition of carbonic anhydrase, a vital enzyme required to maintain pH conditions in bacterial cells (Capasso and Supuran, 2015; Joseph et al., 2011; Alafeefy et al., 2015). Alternatively, the M. microti strain investigated here may possess the ability to synthesize folate, which is inhibited by sulfonamide antibiotics (Davis et al., 2003). The tested fluoroquinolone, macrolide, and tetracycline antibiotics inhibited the growth of M. microti at levels similar to previous reports for Mycoplasma spp. (Table 1, Table S1 in the SI). These findings confirmed that the unexpected inhibition of M. microti by sulfonamides was not an artifact of the culture. Based on these aggregate results, M. microti was highly susceptible to sulfonamide antibiotics for the microdilution and incubation conditions employed in this study, providing an opportunity to greatly improve the sensitivity of antimicrobial activity analysis of sulfonamides.

The chemical structures of sulfamethazine, sulfamerazine, and sulfadiazine differ by the dimethylpyrimidine, methylpyrimidine, and pyrimidine moieties, respectively, at the sulfonamide pharmacophore (Fig. S1 in the SI). Molecular docking studies have confirmed that these minor structural changes affect sulfonamide binding to the functional residues of dihydropteroate synthase (Achari et al., 1997; Hain et al., 2016; Soriano-Correa et al., 2018). The removal of a methyl group from sulfamethazine (to form sulfamerazine) decreased the potency against E. coli  $(IC_{50} = 9.63 \pm 1.48 \text{ mg L}^{-1} \text{ to } IC_{50} = 19.4 \pm 1.3 \text{ mg L}^{-1},$ respectively), but removal of the second methyl group from the pyrimidine ring (to form sulfadiazine) increased the potency (IC50  $=4.76\pm0.23$  mg L<sup>-1</sup>). Interestingly, sulfamethazine was less potent than sulfamerazine for M. microti, but the IC50 parameters of sulfamerazine and sulfadiazine were similar. The differences in the order of antimicrobial potency for sulfonamides with E. coli and M. microti may support alternative mechanisms of action (as suggested above), although additional investigation is needed to confirm these phenomena.

Sulfacetamide and sulfamethoxazole have acetyl and methyl iso-xazole groups, respectively, located at the pharmacophore. Table 1 shows that the  $\rm IC_{50}$  values of sulfacetamide and sulfamethoxazole for *E. coli* were higher than two of the pyrimidine-containing sulfonamides, sulfamethazine and sulfadiazine. However, sulfamethoxazole exhibited the lowest  $\rm IC_{50}$  parameters (*i.e.*, highest potency) for *M. microti* and *P. fluorescens*. The  $\rm IC_{50}$  of sulfacetamide was higher than the other sulfonamides for *M. microti*, but not *P. fluorescens*. The *M. microti* results agree with previous computational studies that calculated stronger

binding of the methyl isoxazole group in sulfamethoxazole to a Staphylococcus aureus dihydropteroate synthase  $(-2.39~\rm kcal~mol^{-1})$  compared to the acetyl group in sulfacetamide  $(-1.42~\rm kcal~mol^{-1})$  (Soriano-Correa et al., 2018); however, the E.~coli and P.~fluorescens results did not follow the same trend. These data not only indicate that the methyl isoxazole and pyrimidine groups confer high antimicrobial activity against M.~microti, but also support application of M.~microti-based assays for investigation of other sulfonamides and sulfonamide-derived transformation products due to the enhanced sensitivity over E.~coli and P.~fluorescens. These findings will bolster opportunities to monitor the residual antimicrobial activity of sulfonamides, which exhibit low  $IC_{50}$  values for traditionally employed bacteria, in environmental applications.

Although sulfamerazine and sulfamethazine did not inhibit *P. fluorescens* growth at the tested concentrations, the pyoverdine inhibition measurements provided insight to the sublethal effects of these antibiotics on *P. fluorescens*. In fact, the EC50 values decreased as methyl groups were sequentially removed from the pyrimidine ring, from  $49.6\pm25.7~\text{mg L}^{-1}$  for sulfamethazine to  $31.6\pm6.0~\text{mg L}^{-1}$  for sulfamerazine to  $6.19\pm2.06~\text{mg L}^{-1}$  for sulfadiazine (Fig. 4, Table 2). These data suggest that *P. fluorescens* is more susceptible to sulfonamides with fewer substitutions on the pyrimidine ring. Given the low potency and solubility limitations of these sulfonamides, this conclusion could not have been obtained through optical density measurements with the conventional CLSI protocol (CLSI, 2016). More discussion of the pyoverdine inhibition results is presented below in Section 3.3.

# 3.2.4. Antimicrobial activity of tetracyclines

The MIC range (145–217 µg L<sup>-1</sup>) recorded for oxytetracycline inhibition of E. coli growth was lower than the 1 mg  $L^{-1}$  (Peng et al., 2014) and 0.5–2.0 mg L<sup>-1</sup> (de Boer et al., 2015) reported by others. This result may stem from the different growth media used in the current study (ISB) and previous reports (Mueller-Hinton broth). Hain et al. (2018) described similar effects of growth medium on the IC50 values of sulfonamide antibiotics. These findings suggest that growth medium optimization, as well as bacteria selection, can be used to improve the sensitivity of antimicrobial activity assays. While no previous reports of oxytetracycline inhibition of M. microti were available, the observed MIC range for oxytetracycline against M. microti (1.95-3.91 mg L<sup>-1</sup>) was similar to previously reported MIC values (1–4 mg  $L^{-1}$ ) for other Mycoplasma spp. (Catania et al., 2019; Heuvelink et al., 2016; Felde et al., 2018). In comparison to E. coli and P. fluorescens, tetracycline antibiotics were less effective against M. microti. The dose-response curves for chlortetracycline are shown in Fig. S6 of the SI for growth inhibition of the three bacteria, as well as pyoverdine inhibition in P. fluorescens; furthermore, the corresponding IC50 and EC50 parameters are summarized in Table 1 and Table 2, respectively.

Tetracycline antibiotics inhibit protein synthesis by preventing aminoacyl-tRNA interaction with the ribosome (Chopra and Roberts, 2001); however, additional mechanisms of action have also been proposed (Chukwudi, 2016). The effectiveness of tetracyclines against viruses and protozoa suggests general inhibition of cellular processes involving double-stranded RNA (Chukwudi, 2016). In addition, the transport of tetracyclines into and out of bacterial cells represents a key aspect of antibiotic potency that is influenced by chemical substitutions to the tetracycline pharmacophore (Chopra and Roberts, 2001; Schnappinger and Hillen, 1996). Compared to chlortetracycline, oxytetracycline was 130% more potent for *E. coli* and 32  $\times$  more potent for M. microti; however, chlortetracycline was 110% more potent than oxytetracycline for P. fluorescens. The chemical structures of oxytetracycline and chlortetracycline differ by hydrogen and chloro groups, respectively, at the C29 and C28 positions and hydroxyl and hydrogen groups, respectively, at the C6 position (Fig. S1 in the SI). The IC<sub>50</sub> values of chlortetracycline (64.1  $\pm$  12.5 mg L<sup>-1</sup>) and oxytetracycline  $(1.96 \pm 0.09 \text{ mg L}^{-1})$  for M. microti indicated that the hydroxy substitution and absence of the chloro group in oxytetracycline resulted in

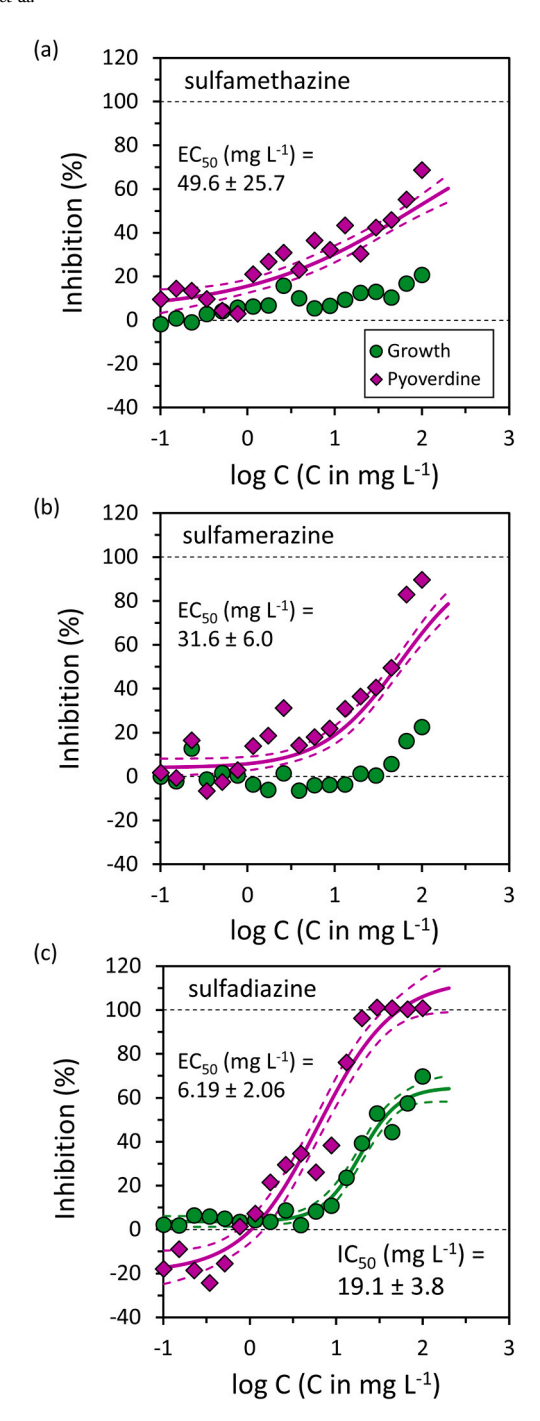


**Fig. 4.** Dose-response curves for (a) sulfamethazine, (b) sulfamerazine, and (c) sulfadiazine growth and pyoverdine inhibition of P. fluorescens. The solid curves are the best fit Hill models, and the dashed curves are the 95% confidence bands. The symbols are the mean inhibition from quadruplicate measurements. The legend in (a) also applies to (b) and (c). The complete list of Hill equation model parameters is reported in Table 1 for growth inhibition and Table 2 for pyoverdine inhibition.

better growth inhibition. The opposite result was observed for P. fluorescens, wherein the IC $_{50}$  parameter of chlortetracycline (119  $\pm$  6  $\mu g$  L $^{-1}$ ) was lower than that of oxytetracycline (245  $\pm$  22  $\mu g$  L $^{-1}$ ). These results likely stem from differences in (i) antibiotic binding to the ribosome or double-stranded RNA or (ii) antibiotic transport into M. microti and P. fluorescens cells (Chopra and Roberts, 2001; Schnappinger and Hillen, 1996).

Overall, the  $IC_{50}$  and  $EC_{50}$  values for tetracycline inhibition of

*P. fluorescens* provided the most sensitivity and, therefore, *P. fluorescens* is recommended for future study of antimicrobial activity of the tetracycline class of antibiotics. Interestingly, the relatively minor chemical substitutions between the tetracycline antibiotics resulted in major differences in antimicrobial activity (Table 1). These results have important consequences for bioassay-based approaches to measuring the activity of environmental transformation products, which often stem from hydrolysis, (de)halogenation, and hydroxylation reactions (Liu et al., 2013; Pei et al., 2016; Xuan et al., 2009; Xu et al., 2012).

## 3.3. Pyoverdine inhibition in P. fluorescens

Bacteriostatic antibiotics, such as fluoroquinolones, macrolides, sulfonamides, and tetracyclines, directly inhibit essential cellular functions to prevent bacteria replication. Sublethal effects are expected to occur at lower antibiotic concentrations than the levels needed for growth inhibition, enabling identification of  $EC_{50}$  values that are lower than the  $IC_{50}$  parameters reported above. This situation presents an opportunity to improve the sensitivity of antimicrobial activity analyses through measurement of specific cellular responses that correlate to growth inhibition outcomes. The benefits of this analysis have already been briefly identified for sulfonamides in Section 3.2.3 and Fig. 4.

Pyoverdine is produced by *Pseudomonas* spp. to scavenge iron and signal virulence factors that strengthen bacteria populations (Dao et al., 1999). Inhibited pyoverdine production suggests that *P. fluorescens* cells have been affected by antibiotics. Depending on the mechanism of action for each antibiotic, cellular processes are disrupted (*e.g.*, transcription by fluoroquinolones (Vancutsem et al., 1990), translation by macrolides (Tenson et al., 2003) and tetracyclines (Chopra and Roberts, 2001), and both transcription and translation by sulfonamides (Petri, 2011)) and decrease pyoverdine levels. Due to its strong fluorescence signal (Fig. S4 in the SI), pyoverdine is easy to measure, often with the same equipment used for optical density measurements. Therefore, the experimental protocols and data analysis employed for growth inhibition were directly translatable to those used for pyoverdine inhibition (Section 2.3).

The  $EC_{50}$  values, related to pyoverdine inhibition, were lower than the  $IC_{50}$  values, corresponding to growth inhibition, for all antibiotics. To better understand the benefits of using pyoverdine inhibition as an antimicrobial activity metric, the  $IC_{50}$  was plotted against the  $EC_{50}$  for all antibiotics in Fig. 5. The  $IC_{50}$ : $EC_{50}$  ratio was close to 1.0 for most of

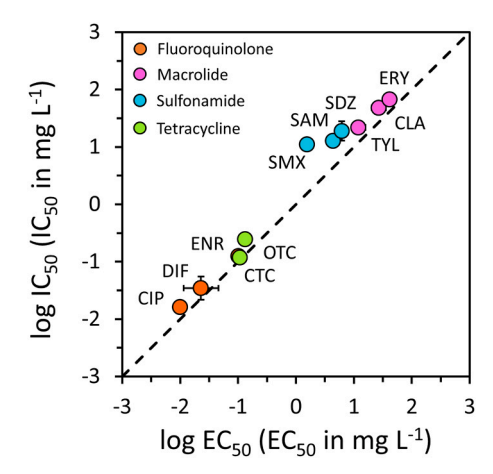


**Fig. 5.** The  $IC_{50}$  values (in log units) for growth inhibition of *P. fluorescens* plotted against the  $EC_{50}$  parameters (in log units) for pyoverdine inhibition in *P. fluorescens*. The symbols are the mean inhibition from quadruplicate measurements, and the error bars (in both directions) represent 95% confidence intervals. Note, sulfamerazine and sulfamethazine were not included in this figure because the  $IC_{50}$  values were outside of the tested concentration range, as indicated in Table 1.

the fluoroquinolones, macrolides, and tetracyclines. These data suggest minor benefits to the sensitivity of measuring antimicrobial activity as pyoverdine inhibition. However, sulfacetamide, sulfadiazine, and sulfamethoxazole exhibited higher ratios of 3.0, 3.1, and 7.2, respectively. Sulfamethoxazole demonstrated the largest difference between the IC<sub>50</sub> for P. fluorescens growth inhibition (11.2  $\pm$  0.5 mg L<sup>-1</sup>) and EC<sub>50</sub> for pyoverdine production (1.55  $\pm$  0.39 mg L<sup>-1</sup>). The order of magnitude difference between the IC50 and EC50 suggested that sulfonamide antibiotics more selectively inhibit pyoverdine production compared to other antibiotics. Generally, sulfonamides inhibit dihydropteroate synthase, which prevents folate production. Folate is essential to several biological functions, including formation of purines and pyrimidines for DNA synthesis and DNA and RNA modification (Naderi and House, 2018). Disruption of transcription and translation processes due to reduced folate production might, therefore, exert stronger sublethal effects compared to the other antibiotic classes that only inhibit transcription (i.e., fluoroquinolones) or translation (i.e., macrolides, tetracyclines). Sulfonamides also inhibit carbonic anhydrase (Joseph et al., 2011; Alafeefy et al., 2015), which may contribute to (or enhance) the observed sublethal effects associated with pyoverdine inhibition. Overall, the utility of pyoverdine inhibition enabled improved sensitivity of antimicrobial activity measurements.

# 3.4. Optimal antibiotic-bacteria pairs

From the above discussion and the summaries of IC50 and EC50 values in Table 1 and Table 2, respectively, the most sensitive bacteria were identified for measurement of antimicrobial activity for the fluoroquinolone, macrolide, sulfonamide, and tetracycline classes of antibiotics. The proposed pairings are as follows: fluoroquinolones with E. coli; macrolides with M. microti; sulfonamides with M. microti; and, tetracyclines with P. fluorescens. Previous studies have mostly employed E. coli to assay fluoroquinolone antibiotics (He et al., 2015; Chu and Fernandes, 1989; Kern et al., 2000; Chow et al., 1988), and so no changes to those protocols are proposed. M. microti were found to be more susceptible to macrolides than the other bacteria. For example, the average macrolide IC<sub>50</sub> for *M. microti* was  $32 \times lower$  than that for *E. coli* and 81  $\times$  lower than that for *P. fluorescens*. These results highlight the increased sensitivity of M. microti for measurement of antimicrobial activity from macrolide antibiotics and, presumably, their degradation products. Similarly, M. microti provided the most sensitive analysis of sulfonamide antibiotics. The average IC50 value for sulfonamides with M. microti was 230% lower than that for E. coli and 280% lower than that for P. fluorescens. Tetracycline antibiotics were generally most potent against P. fluorescens, which has been used in a few previous reports to measure antimicrobial activity (Voigt et al., 2019; Peng et al., 2014). The average IC<sub>50</sub> value for tetracyclines with P. fluorescens was 30% lower than that for E. coli and 180 × lower than that for M. microti; however, the sensitivity of antimicrobial activity analysis can be further improved through measurement of pyoverdine inhibition since the average EC<sub>50</sub> was 52% lower than the IC<sub>50</sub> for P. fluorescens and 90% lower than the IC50 for E. coli. For this reason, the pyoverdine inhibition assay with P. fluorescens is recommended for tetracycline antibiotics.

Use of the antibiotic-bacteria pairs identified above will improve the sensitivity of antimicrobial activity measurements via microdilution protocols. However, the trends in  $IC_{50}$  values were not conserved between the three bacteria, suggesting that analysis of antimicrobial activity with multiple bacteria may provide additional insight into unique interactions between antibiotics, their environmental transformation products, and bacteria. For example, the lowest  $IC_{50}$  values (highest sensitivity) for sulfamerazine and sulfadiazine were identified for M. microti; however, these values were comparable (i.e.,  $2.48 \pm 0.17$  and  $2.58 \pm 0.30$  mg  $L^{-1}$ , respectively) and did not provide insight into the impacts of structural changes on antimicrobial activity. The  $EC_{50}$  values recorded from fluorescence measurements in P. fluorescens highlighted that the loss of a methyl group from sulfamerazine to form sulfadiazine

increased pyoverdine inhibition by 4.1  $\times$ , suggesting stronger sublethal effects of sulfadiazine. Such analysis is expected to provide unique benefits with respect to antimicrobial activity analysis of environmental transformation products for sulfonamides and other antibiotics.

# 4. Conclusion

The sensitivity of the antimicrobial activity assay was improved through informed bacteria selection practices. It is important to note that the sensitivity of antimicrobial activity analysis for fluoroquinolone, macrolide, sulfonamide, and tetracycline antibiotics might be further improved by evaluation of other bacteria species or sublethal targets. The current study focused on three bacteria species that were hypothesized to demonstrate improvements for the antibiotics of concern, but a high-throughput approach may elucidate even greater advantages from other bacteria. Furthermore, deeper analyses of antibiotic-bacteria interactions (e.g., antibiotic transport into the cell, antibiotic binding to biological targets) may inform new strategies for selection of the most sensitive organisms. Unlike clinical settings, where pharmacologists develop new antibiotics to improve inhibition of specific bacteria, optimization of antimicrobial activity assays for environmental applications should involve broad-scale testing of which organisms provide the most sensitive response to certain antibiotics. Higher sensitivity will enable deployment of residual antimicrobial activity assays under the environmentally-relevant conditions needed to identify concerns associated with antibiotics and their degradation products. Future deployment of the reported methods in real wastewater is suggested to confirm accuracy and sensitivity in complex waste streams.

### CRediT authorship contribution statement

Ethan Hain: Conceptualization, data curation, formal analysis, investigation, methodology, validation, visualization, writing – original draft, writing – review & editing. Hollie Adejumo: Conceptualization, methodology, writing – review & editing. Bridget Anger: Investigation, writing – review & editing. Joseph Orenstein: Investigation, writing – review & editing. Lee Blaney: Conceptualization, funding acquisition, project administration, resources, supervision, validation, visualization, writing – original draft, writing – review & editing.

# **Declaration of Competing Interest**

The authors declare that they have no known competing financial interests or personal relationships that could have appeared to influence the work reported in this paper.

#### Acknowledgments

The authors gratefully acknowledge funding from the NSF Environmental Engineering program (#1510420) and the UMBC Undergraduate Research Award program.

# Appendix A. Supporting information

Supplementary data associated with this article can be found in the online version at doi:10.1016/j.jhazmat.2021.125686.

# References

Achari, A., Somers, D.O., Champness, J.N., Bryant, P.K., Rosemond, J., Stammers, D.K., 1997. Crystal structure of the anti-bacterial sulfonamide drug target dihydropteroate synthase. Nat. Struct. Biol. 4, 490–497.

Alafeefy, A.M., Ceruso, M., Al-Tamimi, A.-M.S., Prete, S.D., Supuran, C.T., Capasso, C., 2015. Inhibition studies of quinazoline-sulfonamide derivatives against the γ-CA (PgiCA) from the pathogenic bacterium, Porphyromonas gingivalis. J. Enzyme Inhib. Med. Chem. 30, 592–596.

- Arraes, F., Carvalho, M.J.Ad, Maranhão, A.Q., Brígido, M.M., Pedrosa, F.O., Felipe, M.S. S., 2007. Differential metabolism of Mycoplasma species as revealed by their genomes. Genet. Mol. Biol. 30, 182–189.
- Baeza, C., Knappe, D.R., 2011. Transformation kinetics of biochemically active compounds in low-pressure UV photolysis and UV/H2O2 advanced oxidation processes. Water Res. 45, 4531–4543.
- Barbosa, M.O., Ribeiro, A.R., Ratola, N., Hain, E., Homem, V., Pereira, M.F.R., Blaney, L., Silva, A.M.T., 2018. Spatial and seasonal occurrence of micropollutants in four Portuguese rivers and a case study for fluorescence excitation-emission matrices. Sci. Total Environ. 644, 1128–1140.
- de Boer, M., Heuer, C., Hussein, H., McDougall, S., 2015. Minimum inhibitory concentrations of selected antimicrobials against Escherichia coli and Trueperella pyogenes of bovine uterine origin. J. Dairy Sci. 98, 4427–4438.
- Brown, D., Talkington, D., Thacker, W., Brown, M., Dillehay, D., Tully, J., 2001. Mycoplasma microti sp. nov., isolated from the respiratory tract of prairie voles (Microtus ochrogaster). Int. J. Syst. Evolut. Microbiol. 51, 409–412.
- Capasso, C., Supuran, C.T., 2015. An overview of the alpha-, beta-and gamma-carbonic anhydrases from Bacteria: can bacterial carbonic anhydrases shed new light on evolution of bacteria? J. Enzyme Inhib. Med. Chem. 30, 325–332.
- Catania, S., Bottinelli, M., Fincato, A., Gastaldelli, M., Barberio, A., Gobbo, F., Vicenzoni, G., 2019. Evaluation of minimum inhibitory concentrations for 154 mycoplasma synoviae isolates from Italy collected during 2012–2017. PLoS One 14, e0224903.
- Chen, P., Blaney, L., Cagnetta, G., Huang, J., Wang, B., Wang, Y., Deng, S., Yu, G., 2019. Degradation of ofloxacin by perylene diimide supramolecular nanofiber sunlight-driven photocatalysis. Environ. Sci. Technol. 53, 1564–1575.
- Chernova, O., Medvedeva, E., Mouzykantov, A., Baranova, N., Chernov, V., 2016. Mycoplasmas and their antibiotic resistance: the problems and prospects in controlling infections. Acta Nat. 8, 24–32.
- Chopra, I., Roberts, M., 2001. Tetracycline antibiotics: mode of action, applications, molecular biology, and epidemiology of bacterial resistance. Microbiol. Mol. Biol. Rev. 65, 232–260.
- Chow, R., Dougherty, T., Fraimow, H., Bellin, E.Y., Miller, M., 1988. Association between early inhibition of DNA synthesis and the MICs and MBCs of carboxyquinolone antimicrobial agents for wild-type and mutant [gyrA nfxB (ompF) acrA] Escherichia coli K-12. Antimicrob. Agents Chemother. 32, 1113–1118.
- Chukwudi, C.U., 2016. rRNA binding sites and the molecular mechanism of action of the tetracyclines. Antimicrob. Agents Chemother. 60, 4433–4441.
- Chu, D., Fernandes, P.B., 1989. Structure-activity relationships of the fluoroquinolones. Antimicrob. Agents Chemother. 33, 131–135.
- CLSI, Performance standards for antimicrobial susceptibility testing, Clinical Laboratory Standards Institute. (2016).
- de Crécy-Lagard, V., El Yacoubi, B., de la Garza, R.D., Noiriel, A., Hanson, A.D., 2007. Comparative genomics of bacterial and plant folate synthesis and salvage: predictions and validations. BMC Genom. 8, 245.
- Dao, K.-H.T., Hamer, K.E., Clark, C.L., Harshman, L.G., 1999. Pyoverdine production by pseudomonas aeruginosa exposed to metals or an oxidative stress agent. Ecol. Appl. 9 441–448
- Davis, R.E., Jomantiene, R., Zhao, Y., Dally, E.L., 2003. Folate biosynthesis pseudogenes, ψ folP and ψ folK, and an O-sialoglycoprotein endopeptidase gene homolog in the phytoplasma genome. DNA Cell Biol. 22, 697–706.
- Dodd, M.C., Kohler, H.-P.E., Gunten, U. v., 2009. Oxidation of antibacterial compounds by ozone and hydroxyl radical: elimination of biological activity during aqueous ozonation processes. Environ. Sci. Technol. 43, 2498–2504.
- Van Epps, A., Blaney, L., 2016. Antibiotic residues in animal waste: occurrence and degradation in conventional agricultural waste management practices. Curr. Pollut. Rep. 2, 135–155.
- Felde, O., Kreizinger, Z., Sulyok, K.M., Hrivnák, V., Kiss, K., Jerzsele, Á., Biksi, I., Gyuranecz, M., 2018. Antibiotic susceptibility testing of Mycoplasma hyopneumoniae field isolates from Central Europe for fifteen antibiotics by microbroth dilution method. PLoS One 13, e0209030.
- Garg, S., Rose Andrew, L., Waite, T.D., 2007. Production of reactive oxygen species on photolysis of dilute aqueous quinone solutions. Photochem. Photobiol. 83, 904–913.
- Goutelle, S., Maurin, M., Rougier, F., Barbaut, X., Bourguignon, L., Ducher, M., Maire, P., 2008. The Hill equation: a review of its capabilities in pharmacological modelling. Fundam. Clin. Pharmacol. 22, 633–648.
- Hacek, D.M., Dressel, D.C., Peterson, L.R., 1999. Highly reproducible bactericidal activity test results by using a modified National Committee for Clinical Laboratory Standards broth macrodilution technique. J. Clin. Microb. 37, 1881–1884.
- Hain, E., Camacho, C.J., Koes, D.R., 2016. Fragment oriented molecular shapes. J. Mol. Graphics Modell. 66, 143–154.
- Hain, E., Wammer, K.H., Blaney, L., 2018. Comment on "Photodegradation of sulfathiazole under simulated sunlight: kinetics, photo-induced structural rearrangement, and antimicrobial activities of photoproducts" by Niu et al.[Water Research 124 2017 576–583]. Water Res. 131, 205–207.
- Heuvelink, A., Reugebrink, C., Mars, J., 2016. Antimicrobial susceptibility of Mycoplasma bovis isolates from veal calves and dairy cattle in the Netherlands. Vet. Microbiol. 189, 1–7.
- He, K., Blaney, L., 2015. Systematic optimization of an SPE with HPLC-FLD method for fluoroquinolone detection in wastewater. J. Hazard. Mater. 282, 96–105.
- He, K., Hain, E., Timm, A., Tarnowski, M., Blaney, L., 2019. Occurrence of antibiotics, estrogenic hormones, and UV-filters in water, sediment, and oyster tissue from the Chesapeake Bay. Sci. Total Environ. 650, 3101–3109.
- He, K., Soares, A.D., Adejumo, H., McDiarmid, M., Squibb, K., Blaney, L., 2015. Detection of a wide variety of human and veterinary fluoroquinolone antibiotics in municipal

- wastewater and wastewater-impacted surface water. J. Pharm. Biomed. Anal. 106, 136–143
- Hopanna, M., Mangalgiri, K., Ibitoye, T., Ocasio, D., Snowberger, S., Blaney, L., 2020.
   UV-254 transformation of antibiotics in water and wastewater treatment processes.
   In: Contaminants of Emerging Concern in Water and Wastewater. Butterworth-Heinemann, pp. 239–297.
- Jepsen, R., He, K., Blaney, L., Swan, C., 2019. Effects of antimicrobial exposure on detrital biofilm metabolism in urban and rural stream environments. Sci. Total Environ. 666, 1151–1160.
- Joseph, P., Ouahrani-Bettache, S., Montero, J.-L., Nishimori, I., Minakuchi, T., Vullo, D., Scozzafava, A., Winum, J.-Y., Köhler, S., Supuran, C.T., 2011. A new β-carbonic anhydrase from Brucella suis, its cloning, characterization, and inhibition with sulfonamides and sulfamates, leading to impaired pathogen growth. Bioorg. Med. Chem. 19, 1172–1178.
- Kannan, K., Kanabar, P., Schryer, D., Florin, T., Oh, E., Bahroos, N., Tenson, T., Weissman, J.S., Mankin, A.S., 2014. The general mode of translation inhibition by macrolide antibiotics. Proc. Nat. Acad. Sci. 111, 15958–15963.
- Karkman, A., Johnson, T.A., Lyra, C., Stedtfeld, R.D., Tamminen, M., Tiedje, J.M., Virta, M., 2016. High-throughput quantification of antibiotic resistance genes from an urban wastewater treatment plant. FEMS Microbiol. Ecol. 92, fiw014.
- Keen, O.S., Linden, K.G., 2013. Degradation of antibiotic activity during UV/H2O2 advanced oxidation and photolysis in wastewater effluent. Environ. Sci. Technol. 47, 13020–13030
- Kern, W., Oethinger, M., Jellen-Ritter, A., Levy, S., 2000. Non-target gene mutations in the development of fluoroquinolone resistance in Escherichia coli. Antimicrob. Agents Chemother. 44, 814–820.
- Koczura, R., Mokracka, J., Jabłońska, L., Gozdecka, E., Kubek, M., Kaznowski, A., 2012. Antimicrobial resistance of integron-harboring Escherichia coli isolates from clinical samples, wastewater treatment plant and river water. Sci. Total Environ. 414, 680-685
- Linde, H.-J., Notka, F., Metz, M., Kochanowski, B., Heisig, P., Lehn, N., 2000. In vivo increase in resistance to Ciprofloxacin in Escherichia coli associated with deletion of the C-terminal part of MarR. Antimicrob. Agents Chemother. 44, 1865–1868.
- Liu, S., Zhao, X.-R., Sun, H.-Y., Li, R.-P., Fang, Y.-F., Huang, Y.-P., 2013. The degradation of tetracycline in a photo-electro-Fenton system. Chem. Eng. J. 231, 441–448.
- Luber, P., Bartelt, E., Genschow, E., Wagner, J., Hahn, H., 2003. Comparison of broth microdilution, E test, and agar dilution methods for antibiotic susceptibility testing of Campylobacter jejuni and Campylobacter coli. J. Clin. Microbiol. 41, 1062–1068.
- Maguna, F.P., Okulik, N.B., Castro, E.A., 2016. Quantitative Structure–Activity Relationships of Antimicrobial Compounds. In: Leszczynski, J. (Ed.), Handbook of Computational Chemistry. Springer Netherlands, Dordrecht, pp. 1–17.
- Mazzei, T., Mini, E., Novelli, A., Periti, P., 1993. Chemistry and mode of action of macrolides. J. Antimicrob. Chemother. 31, 1–9.
- McCormack, W.M., 1993. Susceptibility of mycoplasmas to antimicrobial agents: clinical implications. Clin. Infect. Dis. 17, S200–S201.
- Melnikov, S., Manakongtreecheep, K., Söll, D., 2018. Revising the structural diversity of ribosomal proteins across the three domains of life. Mol. Biol. Evol. 35, 1588–1598.
- Meyer, J.-M., 2000. Pyoverdines: pigments, siderophores and potential taxonomic markers of fluorescent Pseudomonas species. Arch. Microbiol. 174, 135–142.
- Mizdal, C.R., Stefanello, S.T., Nogara, P.A., Soares, F.A.A., de Lourenço Marques, L., de Campos, M.M.A., 2018. Molecular docking, and anti-biofilm activity of goldcomplexed sulfonamides on Pseudomonas aeruginosa. Microb. Pathog. 125, 393-400
- Mouneimné, H., Robert, J., Jarlier, V., Cambau, E., 1999. Type II topoisomerase mutations in ciprofloxacin-resistant strains of Pseudomonas aeruginosa. Antimicrob. Agents Chemother. 43, 62–66.
- Naderi, N., House, J.D., 2018. Recent developments in folate nutrition. In: Advances in Food and Nutrition Research. Elsevier, pp. 195–213.
- Pei, J., Yao, H., Wang, H., Ren, J., Yu, X., 2016. Comparison of ozone and thermal hydrolysis combined with anaerobic digestion for municipal and pharmaceutical waste sludge with tetracycline resistance genes. Water Res. 99, 122–128.
- Peng, F.J., Zhou, L.J., Ying, G.G., Liu, Y.S., Zhao, J.L., 2014. Antibacterial activity of the soil-bound antimicrobials oxytetracycline and ofloxacin. Environ. Toxicol. Chem. 33, 776–783.
- Peterson, L.R., 2001. Quinolone molecular structure-activity relationships: what we have learned about improving antimicrobial activity. Clin. Infect. Dis. 33, S180–S186.
- Petri, W., 2011. Sulfonamides, trimethoprim-sulfamethoxazole, quinolones, and agents for urinary tract infections. Goodman & Gilman's The Pharmacological Basis of Therapeutics. 12th. McGraw-Hill, New York, pp. 1463–1476.
- Pomati, F., Orlandi, C., Clerici, M., Luciani, F., Zuccato, E., 2008. Effects and interactions in an environmentally relevant mixture of pharmaceuticals. Toxicol. Sci. 102, 129–137.
- Postigo, C., Richardson, S.D., 2014. Transformation of pharmaceuticals during oxidation/disinfection processes in drinking water treatment. J. Hazard. Mater. 279, 461–475.
- Reller, L.B., Weinstein, M., Jorgensen, J.H., Ferraro, M.J., 2009. Antimicrobial susceptibility testing: a review of general principles and contemporary practices. Clin. Infect. Dis. 49, 1749–1755.
- Scales, B.S., Dickson, R.P., LiPuma, J.J., Huffnagle, G.B., 2014. Microbiology, genomics, and clinical significance of the Pseudomonas fluorescens species complex, an unappreciated colonizer of humans. Clin. Microbiol. Rev. 27, 927–948.
- Schnappinger, D., Hillen, W., 1996. Tetracyclines: antibiotic action, uptake, and resistance mechanisms. Arch. Microbiol. 165, 359–369.
- Schumacher, A., Vranken, T., Malhotra, A., Arts, J., Habibovic, P., 2018. In vitro antimicrobial susceptibility testing methods: agar dilution to 3D tissue-engineered models. Europ. J. Clin. Microbiol. Infect. Dis. 37, 187–208.

- Sekizuka, T., Inamine, Y., Segawa, T., Hashino, M., Yatsu, K., Kuroda, M., 2019. Potential KPC-2 carbapenemase reservoir of environmental Aeromonas hydrophila and Aeromonas caviae isolates from the effluent of an urban wastewater treatment plant in Japan. Environ. Microbiol. Rep. 11, 589–597.
- Snowberger, S., Adejumo, H., He, K., Mangalgiri, K.P., Hopanna, M., Soares, A.D., Blaney, L., 2016. Direct photolysis of fluoroquinolone antibiotics at 253.7 nm: specific reaction kinetics and formation of equally potent fluoroquinolone antibiotics. Environ. Sci. Technol. 50, 9533–9542.
- Soriano-Correa, C., Barrientos-Salcedo, C., Francisco-Márquez, M., Sainz-Díaz, C.I., 2018. Computational study of substituent effects on the acidity, toxicity and chemical reactivity of bacteriostatic sulfonamides. J. Mol. Graph. Model. 81, 116–124.
- Su, H.-C., Liu, Y.-S., Pan, C.-G., Chen, J., He, L.-Y., Ying, G.-G., 2018. Persistence of antibiotic resistance genes and bacterial community changes in drinking water treatment system: from drinking water source to tap water. Sci. Total Environ. 616, 453-461
- Szabó, L., Szabó, J., Illés, E., Kovács, A., Belák, Á., Mohácsi-Farkas, C., Takács, E., Wojnárovits, L., 2017. Electron beam treatment for tackling the escalating problems of antibiotic resistance: eliminating the antimicrobial activity of wastewater matrices originating from erythromycin. Chem. Eng. J. 321, 314–324.
- Tahrani, L., Van Loco, J., Ben Mansour, H., Reyns, T., 2016. Occurrence of antibiotics in pharmaceutical industrial wastewater, wastewater treatment plant and sea waters in Tunisia. J. Water Health 14, 208–213.
- Tappe, W., Zarfl, C., Kummer, S., Burauel, P., Vereecken, H., Groeneweg, J., 2008. Growth-inhibitory effects of sulfonamides at different pH: dissimilar susceptibility patterns of a soil bacterium and a test bacterium used for antibiotic assays. Chemosphere 72, 836–843.
- Tenson, T., Lovmar, M., Ehrenberg, M., 2003. The mechanism of action of macrolides, lincosamides and streptogramin B reveals the nascent peptide exit path in the ribosome. J. Mol. Biol. 330, 1005–1014.
- Vancutsem, P., Babish, J., Schwark, W., 1990. The fluoroquinolone antimicrobials: structure, antimicrobial activity, pharmacokinetics, clinical use in domestic animals and toxicity. Cornell Vet. 80, 173–186.
- Vergalli, J., Dumont, E., Cinquin, B., Maigre, L., Pajovic, J., Bacqué, E., Mourez, M., Réfrégiers, M., Pagès, J.-M., 2017. Fluoroquinolone structure and translocation flux across bacterial membrane. Sci. Rep. 7, 1–8.
- Voigt, M., Bartels, I., Nickisch-Hartfiel, A., Jaeger, M., 2019. Determination of minimum inhibitory concentration and half maximal inhibitory concentration of antibiotics

- and their degradation products to assess the eco-toxicological potential. Toxicol. Environ. Chem.  $101,\,315-338.$
- Voigt, M., Bartels, I., Nickisch-Hartfiel, A., Jaeger, M., 2018. Elimination of macrolides in water bodies using photochemical oxidation. AIMS Environ. Sci. 5, 372–378.
- Voigt, M., Bartels, I., Nickisch-Hartfiel, A., Jaeger, M., 2017. Photoinduced degradation of sulfonamides, kinetic, and structural characterization of transformation products and assessment of environmental toxicity. Toxicol. Environ. Chem. 99, 1304–1327.
- Wammer, K.H., Lapara, T.M., McNeill, K., Arnold, W.A., Swackhamer, D.L., 2006. Changes in antibacterial activity of triclosan and sulfa drugs due to photochemical transformations. Environ. Toxicol. Chem. Int. J. 25, 1480–1486.
- Wasserman, A.E., 1965. Absorption and fluorescence of water-soluble pigments produced by four species of Pseudomonas. Appl. Environ. Microbiol. 13, 175–180.
- Wei, R., Dou, H., Wang, L., Li, D., Tian, X., Li, J., Li, S., Xin, D., 2019. In vitro susceptibility test of Xiao'er Feire Kechuan Oral Solution to Mycoplasma pneumoniae. Medicine 98. e16070.
- Wetzstein, H.-G., 2005. Comparative mutant prevention concentrations of pradofloxacin and other veterinary fluoroquinolones indicate differing potentials in preventing selection of resistance. Antimicrob. Agents Chemother. 49, 4166–4173.
- Winissorn, W., Tribuddharat, C., Naenna, P., Leelarasamee, A., Pongpech, P., 2013. Fluoroquinolone resistance and effect of qnrA integron cassettes in Escherichia coli clinical isolates in a university hospital. J. Infect. Dis. Antimicrob. Agents 30, 15–25.
- Witebsky, F.G., Maclowry, J., French, S., 1979. Broth dilution minimum inhibitory concentrations: rationale for use of selected antimicrobial concentrations. J. Clin. Microbiol. 9, 589–595.
- Xuan, R., Arisi, L., Wang, Q., Yates, S.R., Biswas, K.C., 2009. Hydrolysis and photolysis of oxytetracycline in aqueous solution. J. Environ. Sci. Health Part B 45, 73–81.
- Xu, B., Zhu, H.-Z., Lin, Y.-L., Shen, K.-Y., Chu, W.-H., Hu, C.-Y., Tian, K.-N., Mwakagenda, S.A., Bi, X.-Y., 2012. Formation of volatile halogenated by-products during the chlorination of oxytetracycline. Water Air Soil Pollut. 223, 4429–4436.
- Zhang, Y., Duan, L., Wang, B., Du, Y., Cagnetta, G., Huang, J., Blaney, L., Yu, G., 2019. Wastewater-based epidemiology in Beijing, China: prevalence of antibiotic use in flu season and association of pharmaceuticals and personal care products with socioeconomic characteristics. Environ. Int. 125, 152–160.
- Zhang, Y., Duan, L., Wang, B., Liu, C.S., Jia, Y., Zhai, N., Blaney, L., Yu, G., 2020. Efficient multiresidue determination method for 168 pharmaceuticals and metabolites: optimization and application to raw wastewater, wastewater effluent, and surface water in Beijing, China. Environ. Pollut. 261, 114113.